

# WEARABLE STRETCHABLE DOUBLE-SIDED MICRO-SUPERCAPACITORS WITH POROUS CONDUCTIVE ELASTOMERS

Yu Song<sup>1,†</sup>, Zijian Song<sup>1,†</sup>, Haotian Chen<sup>1,2</sup>, Xuexian Chen<sup>1,2</sup>, Hang Guo<sup>1,2</sup>, Hanxiang Wu<sup>1</sup>, Xiaoliang Cheng<sup>1</sup>, and Haixia Zhang<sup>1,2,\*</sup>

<sup>1</sup>National Key Laboratory of Science and Technology on Micro/Nano Fabrication, Institute of Microelectronics, Peking University, Beijing, CHINA

<sup>2</sup>Academy for Advanced Interdisciplinary Studies, Peking University, Beijing, CHINA

## ABSTRACT

In this paper, we present a facile fabrication for wearable stretchable micro-supercapacitors with porous carbon nanotube-polydimethylsiloxane (CNT-PDMS) conductive elastomer, which combines laser cutting with electrolyte transferring process. Taking advantage of porous structure with large surface area and highly conductive elastomer, such device demonstrates great areal capacitance, reliable flexibility and cycling stability after 2,000 charging-discharging cycles. Meanwhile, with in-planar and parallel layout, the electrochemical performance of the double-sided micro-supercapacitor (D-MS-C) is greatly enhanced compared with single-sided MSC. Therefore, the wearable D-MS-C shows promising potentials in the wearable electronics and smart energy systems.

## INTRODUCTION

Nowadays, personal electronics are achieving great attention, which brings in the rapid development of matched energy devices [1]. As two main components of smart energy systems [2], high efficiency energy harvester from the environment and stable integrated energy storage device have been significantly advanced. For energy conversion methods, triboelectric nanogenerator [3,4], piezoelectric nanogenerator [5,6] and self-charging power unit [7,8] are considerable approaches. As another critical component, supercapacitor is considered to have wide potential applications among available energy storage devices, which possesses cycling stability, fast charging rates and bio-compatibility [9,10].

Unfortunately, conventional supercapacitor with sandwiched structure limits its application in on-chip device and microsystem, because the miniaturized electronics and mechanical devices desire energy components with similar dimensions compared with other elements [11]. Recently, the in-planar supercapacitor, also called micro-supercapacitor (MSC) [12-14], has drawn great attentions in micro energy fields. As an emerging member in supercapacitor's family, MSC with in-planar layout can render the diffusion length and promote the procedure of ion exchange. With the elimination of the separator, the total thickness of the device could be great decreased, where MSC could allow more active materials loaded per unit and maintain excellent electrochemical performance, promoting the integration of power sources with the electronic circuit [15,16].

However, normal researches on MSCs mainly focus on the performance improvement [17], and ignore the cost, ease of preparation and device integration. Meanwhile, the patterning of the interdigital MSC is commonly employed

with lithography process, which seems costly and possibly damages the electrode materials during the etching stage. Therefore, it remains a challenge to obtain MSC with excellent stability, flexibility in a low-cost and easy process at the same time.

Herein, to address the above issues, we present a facile and integrated fabrication to develop a wearable D-MS-C through the laser patterning and electrolyte transferring process. In our design, the solid-state electrolyte serves as both ion reservoir and substrate, which could decrease the total thickness and enhance flexibility, and porous conductive elastomer demonstrates ideal electrochemical performance. It could be further improved through the double-sided parallel connection, which shows potential candidate in integrated energy storage device and low-power electronic systems.

## EXPERIMENTAL METHODS

Fig. 1 shows the schematic diagram of the D-MS-C and latent integration into the energy storage bracelet with stretchable substrate. Such device includes the in-planar MSCs, Ecoflex substrate and magnets. For the individual MSC device, it is worth mentioning that the electrolyte also serves as the basic substrate and interdigital electrodes with porous CNT-PDMS conductive elastomer serve as anode and cathode. The thickness of whole device could be greatly decreased with the electrolyte-substrate layout, which performs good flexibility and portability.

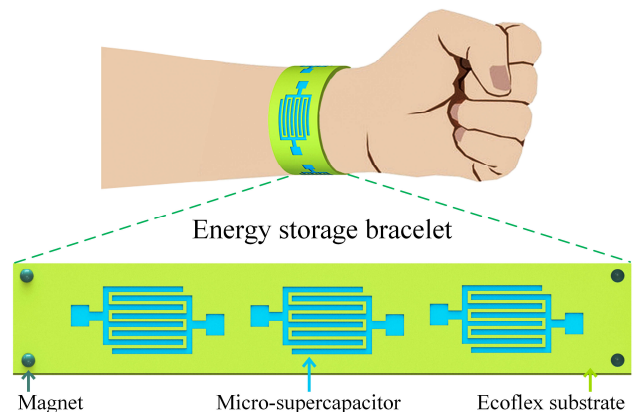


Figure 1: Schematic diagram of the D-MS-Cs as the potential energy storage bracelet and top view of the structure.

## Material preparation

The preparation of the CNT-PDMS mixture is essential for the fabrication process shown in Fig. 2. In our process, 3 g elastomer of commercial PDMS (Sylgard 184, Dow Corning Co.) and 600 mg of CNTs (Boyu Co.) are firstly

dissolved in toluene at a polymer/solvent concentration of 20%. The mixture is magnetic stirred for 4 h at the room temperature until the CNTs are mixed into PDMS thoroughly with the help of toluene.



**Figure 2:** Fabrication process of the CNT-PDMS mixture with stirring CNT, PDMS and toluene to obtain CNT-PDMS elastomer and further adding sugar to prepare CNT-PDMS mixture.

Then the mixture is poured into a culture dish to evaporate residual toluene. Meanwhile, 300 mg cross-linker of PDMS and 15 g sugar are added with 0.5 h magnetic stirring until toluene is totally removed. Finally, the CNT-PDMS mixture with sugar could be obtained after cured at 100 °C for 2 h.

As for the solid-state electrolyte, it is prepared by adding polyvinyl alcohol (PVA) powder (6 g) into H<sub>3</sub>PO<sub>4</sub> aqueous solution (6 g H<sub>3</sub>PO<sub>4</sub> into 60 ml deionized water). The whole mixture is heated to 85°C under vigorous stirring until the solution becomes clear.

### Fabrication of MSC device

The fabrication process of the MSC device is demonstrated in Fig. 3. Firstly, PMMA mold is patterned with designed interdigital structure through laser-cutting process (Fig. 3(a)). Then the prepared CNT-PDMS mixture with sugar is filled into the grooves (Fig. 3(b)). Next, gel electrolyte consisting of PVA and H<sub>3</sub>PO<sub>4</sub> is spray coated among the PMMA surface (Fig. 3(c)). The device is completely dried in a regular oven at 45°C for 12 h to fully vaporize the excess water.

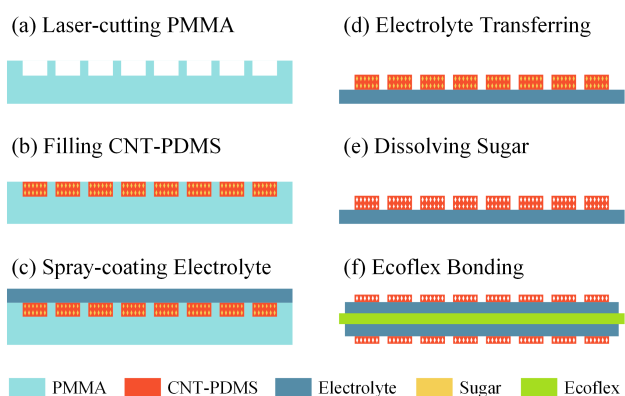


**Figure 3:** Fabrication process of the D-MSD. (a) Laser patterning PMMA with interdigital structure, (b) filling CNT-PDMS into the grooves, (c) spray-coating electrolyte on the surfaces, (d) transferring the CNT-PDMS mixture by the electrolyte, (e) dissolving sugar to form porous structure, and (f) assembling on both sides of Ecoflex to obtain D-MSD.

After the above layers is peeled off from the PMMA substrate, the CNT-PDMS mixture could be easily transferred to the dried electrolyte film without further substrate (Fig. 3(d)). To promote the contact area and ion

exchange, the sugar is dissolved in the water (Fig. 3(e)). Finally, several MSCs are integrated on the both sides of Ecoflex substrate with alignment and the D-MSD is successfully prepared (Fig. 3(f)).

### Measurement and Analysis

The morphologies, structure of each layer and the interdigital MSC are all analyzed using a scanning electron microscope (SEM) (Quanta 600F, FEI Co.). All of the electrochemical tests of the MSCs are carried out by a two-electrode system using CHI660C (CH instrument) electrochemical workstation at room temperature.

## RESULTS AND DISCUSSION

### Optical and SEM analysis

With the proposed process, the flexible MSC with interdigital electrodes has been fabricated (Fig. 4(a)). Obviously, the MSC owns a well-defined shape, which could be easily rolled up and meet the demands in portable electronics. In addition, SEM images in Fig. 4(b)-4(c) clearly demonstrate the morphologies of sugar powders and porous CNT-PDMS structure, where the sugar possesses average length of 30 μm and brings in the uniform pores after dissolving process. The cross-section SEM image of the device in Fig. 4(d) shows the detailed structure composed of electrode layer and solid-state electrolyte film. It proves that the electrolyte is penetrated into the electrode, which could enhance the ion exchange.

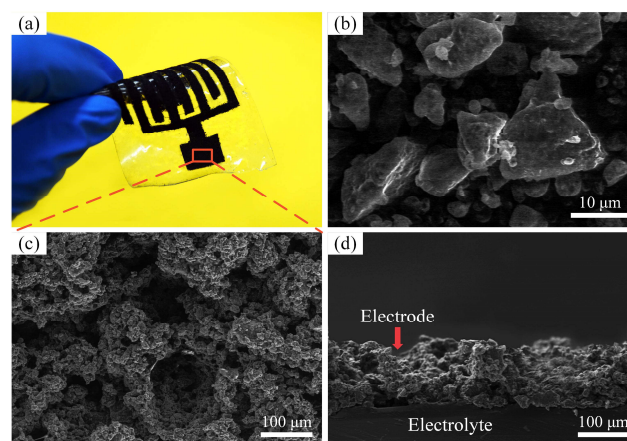


**Figure 4:** (a) Digital image of the flexible MSC device. SEM images of (b) sugar powders, (c) porous CNT-PDMS and (d) the cross-section of the device.

### Electrochemical analysis

As for the electrochemical performance of the flexible MSC, the device is carefully evaluated through cyclic voltammetry (CV), galvanostatic charge-discharge (GCD), Ragone plots and cycling stability via the electrochemical workstation. At first, CV curves with the scan rates from 10 mV/s to 200 mV/s are recorded at a stable potential window between 0 and 1 V. As shown in Fig. 5(a), quasi-rectangular shapes could be observed due to the characteristic of the carbon-based materials, proving the ideal double-layer electrochemical behavior.

Then GCD test is also measured in Fig. 5(b), where the typical GCD curves are performed, the charging currents of which are from 4 μA to 12 μA. Discharging profiles of

the fabricated MSC are dependent on the applied charging-discharging currents. Evidently, the charging curves are symmetrical with their corresponding discharging counterparts, as well as their excellent linear voltage-time profiles, demonstrating good electrochemical behavior of the device.

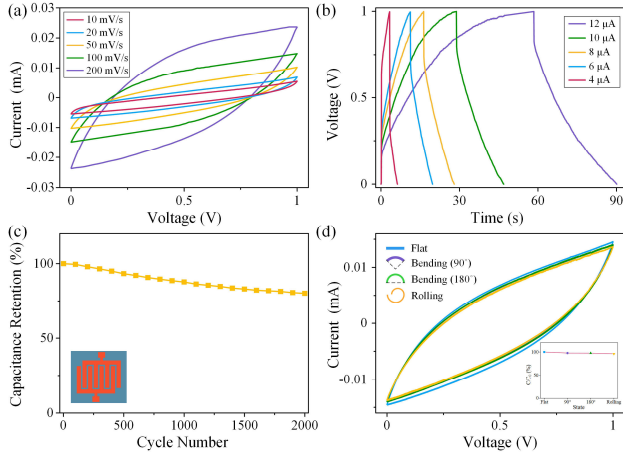


**Figure 5: Electrochemical behavior of the S-MSC.** (a) CV curves, (b) GCD curves, (c) cycling stability and (d) CV curves under different bending conditions.

Fig. 5(c) shows the cycling stability of the MSC with interdigital electrodes during the repetitive charging-discharging cycles (100 mV/s). Obviously, more than 80% of the initial capacitance is maintained after 2,000 cycles of CV test.

Furthermore, to evaluate the feasibility as the energy storage component for flexible electronics, the MSC device is tested under different bending conditions. From Fig. 5(d), there are negligible changes of the CV curves under bending or rolling states, which greatly illustrates the flexibility of the MSC device. Therefore, such flexible MSC device proves stable and reliable electrochemical performance, which could satisfy the needs of self-powered systems.

### Double-sided MSC design

In order to improve the capacitance and energy per unit area, MSCs are fabricated on both sides of an Ecoflex film and connected in parallel to form the double-sided MSC (D-MSC). To protect the D-MSC from external impact and prevent degradation of the electrolyte in air, the whole MSC is encapsulated with a thin Ecoflex film. Detailed electrochemical performance comparison between single-sided MSC (S-MSC) and D-MSC is shown in Fig. 6. As shown in Fig. 6(a)-(b), both the CV curves (100 mV/s) and the GCD curves (10  $\mu$ A) could be doubled *via* the parallel connection of D-MSC.

Besides, as the areal capacitance is the most precise characterization for evaluating the charge-storage capacity of MSC, the areal capacitance is achieved according to the following equation (1) based on the CV curves of both the S-MSC and D-MSC:

$$C_A = \frac{Q}{A \cdot \Delta V} = \frac{1}{k \cdot A \cdot \Delta V} \int_{V_1}^{V_2} I(V) dV \quad (1)$$

where,  $C_A$  is the areal capacitance,  $I(V)$  is the discharge

current function,  $k$  is the scan rate,  $A$  is the area of the MSC and  $\Delta V$  is the potential window during the discharge process, where  $V_1$  and  $V_2$  are maximum and minimum voltage values, respectively. Fig. 6(c) compares the areal capacitance of S-MSC and D-MSC at various scan rates. With the scan rate of 10 mV/s, the D-MSC and S-MSC could achieve the maximum areal capacitance of 140  $\mu$ F/cm<sup>2</sup> and 63  $\mu$ F/cm<sup>2</sup>, respectively, which decreases slightly with the increase of the scan rate. As a result, the electrochemical performance could be further enhanced through the D-MSC design. Meanwhile, such device could withstand the charging-discharging process without significant degradation in areal capacitance even at high scan rate, showing a stable and excellent electrochemical performance.

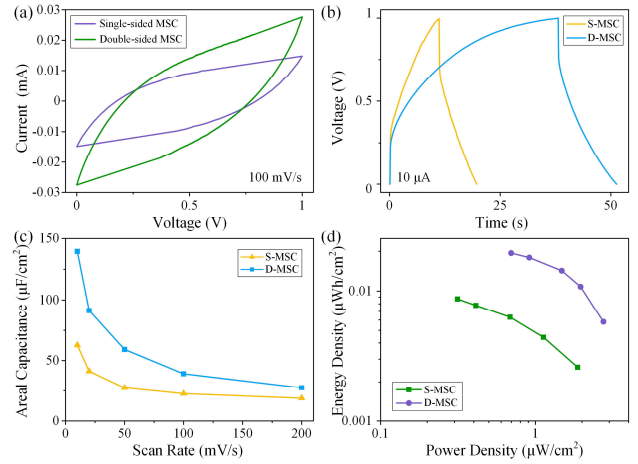


**Figure 6: Electrochemical performance comparison between S-MSC and D-MSC.** (a) CV curves at 100 mV/s, (b) GCD curves at 10  $\mu$ A, (c) calculated areal capacitance and (d) Ragone plots.

Subsequently, the areal energy and power density of S-MSC and D-MSC are calculated from CV curves at a voltage scan rate of 10 to 200 mV/s shown in Fig. 6(d). Both of them at initial state could be achieved by the following equations with the size of 7.8 cm<sup>2</sup>:

$$E = \frac{1}{2 \times 3600} C_A (\Delta V)^2 \quad (2)$$

$$P = \frac{E}{\Delta t} \times 3600 \quad (3)$$

where,  $C_A$  is the areal capacitance of the MSC which could be achieved through eq. 1,  $\Delta t$  is the discharging time,  $E$  is the energy density and  $P$  is the power density, respectively. The highest energy density of the D-MSC is 0.02  $\mu$ Wh/cm<sup>2</sup> at the scan rate of 10 mV/s, while the highest power density is 2.75  $\mu$ W/cm<sup>2</sup> at the scan rate of 200 mV/s. Obviously, both of them vary slightly with the increase of scan rate and D-MSC shows better performance compared with S-MSC.

## CONCLUSIONS

In summary, we propose a wearable double-sided MSC based on conductive elastomer with great characteristic of flexibility, stability and lightweight. Utilizing the laser patterning and electrolyte transferring process, this facile and scalable procedure could be easily integrated into portable electronics. The MSC is

configured with porous CNT-PDMS conductive elastomer as active materials, PVA/H<sub>3</sub>PO<sub>4</sub> as substrate and solid-state electrolyte. Meanwhile, the entire device shows great electrochemical behavior with reliable areal capacitance and cycling stability, attributed to the fact that porous elastomer owns large surface area and high conductivity. Moreover, with in-planar and parallel layout, the electrochemical performance of the D-MSC is greatly enhanced compared with S-MSC, which could be further integrated into energy storage bracelet with stretchable Ecoflex substrate. Therefore, such wearable D-MSC device performs significant advantages in MEMS-based technology, large-scale fabrication and flexible miniaturized energy systems.

## ACKNOWLEDGEMENTS

This work is supported by the National Natural Science Foundation of China (Grant No. 61674004), and the Beijing Natural Science Foundation of China (Grant No. 4141002).

## REFERENCES

- [1] Y. Song, H. Chen, Z. Su, X. Chen, L. Miao, J. Zhang, X. Cheng and H. Zhang, "Highly compressible integrated supercapacitor-piezoresistance-sensor system with CNT-PDMS sponge for health monitoring", *Small*, vol. 13, 1702091, 2017.
- [2] J. Chen, Y. Huang, N. Zhang, H. Zou, R. Liu, C. Tao, X. Fan and Z. Wang, "Micro-cable structured textile for simultaneously harvesting solar and mechanical energy", *Nat. Energy*, vol. 1, 16138, 2016.
- [3] X. Zhang, M. Han, B. Meng and H. Zhang, "High performance triboelectric nanogenerators based on large-scale mass-fabrication technologies", *Nano Energy*, vol. 11, pp. 304-322, 2015.
- [4] B. Meng, W. Tang, Z. Too, X. Zhang, M. Han, W. Liu and H. Zhang, "A transparent single-friction-surface triboelectric generator and self-powered touch sensor", *Energy Environ. Sci.*, vol. 6, pp. 3235-3240, 2013.
- [5] M. Han, X. Zhang, B. Meng, W. Liu, W. Tang, X. Sun, W. Wang and H. Zhang, "r-Shaped hybrid nanogenerator with enhanced piezoelectricity", *ACS Nano*, vol. 7, pp. 8554-8560, 2013.
- [6] Q. Zhong, J. Zhong, X. Cheng, X. Yao, B. Wang, W. Li, N. Wu, K. Liu, B. Hu, and J. Zhou, "Paper-based active tactile sensor array", *Adv. Mater.*, vol. 27, pp. 7130-7136, 2015.
- [7] Y. Song, X. Cheng, H. Chen, J. Huang, X. Chen, M. Han, Z. Su, B. Meng, Z. Song and H. Zhang, "Integrated self-charging power unit with flexible supercapacitor and triboelectric nanogenerator", *J. Mater. Chem. A*, vol. 4, pp. 14298-14306, 2016.
- [8] Y. Song, J. Zhang, H. Guo, X. Chen, Z. Su, H. Chen, X. Cheng and H. Zhang, "All-fabric-based wearable self-charging power cloth", *Appl. Phys. Lett.*, vol. 111, 073901, 2017.
- [9] P. Simon and Y. Gogotsi, "Materials for electrochemical capacitors", *Nat. Mater.*, vol. 7, pp. 845-854, 2008.
- [10] X. Lu, M. Yu, G. Wang, Y. Tong and Y. Li, "Flexible solid-state supercapacitors: design, fabrication and applications", *Energy Environ. Sci.*, vol. 7, pp. 2160-2181, 2014.
- [11] Y. Song, X. Cheng, H. Chen, M. Han, X. Chen, J. Huang, Z. Su and H. Zhang, "Highly compression-tolerant folded carbon nanotube/paper as solid-state supercapacitor electrode", *Micro Nano Lett.*, vol. 11, pp. 586-590, 2016.
- [12] X. Pu, M. Liu, L. Li, S. Han, X. Li, C. Jiang, C. Du, J. Luo, W. Hu and Z. Wang, "Wearable textile-based in-plane microsupercapacitors", *Adv. Energy Mater.*, vol. 6, 1601254, 2016.
- [13] D. Kim, G. Lee, D. Kim, J. Yun, S. Lee and J. Ha, "High performance flexible double-sided microsupercapacitors with an organic gel electrolyte containing a redox-active additive", *Nanoscale*, vol. 8, pp. 15611-15620, 2016.
- [14] Y. Song, X. Chen, J. Zhang, X. Cheng and H. Zhang, "Freestanding micro-supercapacitor with interdigital electrodes for low-power electronic systems", *J. Microelectromech. Syst.*, vol. 26, pp. 1055-1062, 2017.
- [15] X. Liu, S. Chen, J. Pu, and X. Wang, "A flexible all-solid-state micro supercapacitor and its application in electrostatic energy management system", *J. Microelectromech. Syst.*, vol. 25, pp. 929-936, 2016.
- [16] J. Yun, Y. Lim, H. Lee, G. Lee, H. Park, S. Hong, S. Lee and J. Ha, "A patterned Graphene/ZnO UV sensor driven by integrated asymmetric microsupercapacitors on a liquid metal patterned foldable paper", *Adv. Funct. Mater.*, vol. 27, 1700135, 2017.
- [17] M. El-Kady and R. Kaner, "Scalable fabrication of high-power graphene micro-supercapacitors for flexible and on-chip energy storage", *Nat. Commun.*, vol. 4, pp. 1475, 2013.

## CONTACT

\*H.X. Zhang, hxzhang@pku.edu.cn

†These authors contribute equally.